

Photometric search for variable stars in young open cluster Berkeley 59

Sneh Lata ^{*}, A. K. Pandey, Maheswar G., Soumen Mondal and Brijesh Kumar

Aryabhata Research Institute of Observational Sciences, Manora Peak, Nainital 263129, Uttarakhand, India

Accepted ———. Received ———;

ABSTRACT

We present time-series photometry of stars located in the extremely young open cluster Berkeley 59. Using the 1.04 m telescope at ARIES, Nainital, we have identified 42 variables in a field of $\sim 13' \times 13'$ around the cluster. The probable members of the cluster are identified using $(V, V - I)$ colour-magnitude diagram and $(J - H, H - K)$ colour-colour diagram. Thirty one variables are found to be pre-main sequence stars associated with the cluster. The ages and masses of pre-main sequence stars are derived from colour-magnitude diagram by fitting theoretical models to the observed data points. The ages of the majority of the probable pre-main sequence variable candidates range from 1 to 5 Myrs. The masses of these pre-main sequence variable stars are found to be in the range of ~ 0.3 to $\sim 3.5 M_{\odot}$ and these could be T Tauri stars. The present statistics reveal that about 90% T Tauri stars have periods < 15 days. The classical T Tauri stars are found to have larger amplitude in comparison to the weak line T Tauri stars. There is an indication that the amplitude decreases with increase of the mass, which could be due to the dispersal of disk of relatively massive stars.

Key words: Open cluster: Berkeley 59 – colour-magnitude diagram: Variables-pre-main sequence stars

1 INTRODUCTION

Variable stars are useful tools to improve our understanding on stellar evolution and structure of stars. Star clusters are unique laboratories to study the stellar evolution as star clusters provide a sample of stars having same age, distance, initial composition and spanning range of masses. Additionally, the light curves of several stars can be produced simultaneously to know the real variable stars among them. Studies of variable stars in star clusters are carried out since several years (Herbst et al. 1994; Edwards et al. 1993; Oliveira & Casali 2008; Grankin et al. 2008). Star clusters have different types of variable stars as stars show variability at various stages of their evolutionary phases.

In the present study, we made a search for variable stars in an extremely young open cluster Berkeley 59 (Be 59). Be 59 is a young cluster and it contains a significant numbers of pre-main sequence (PMS) stars i.e, stars evolving from their birthline to the main-sequence (MS). This cluster ($\alpha_{2000} = 00^h 02^m 13^s$, $\delta_{2000} = +67^{\circ} 25' 11''$, $l = 118^{\circ}.22$, $b = 5^{\circ}.00$) is located at the centre of OB4 stellar association surrounded by HII region, Sharpless region S171 (Yang & Fukui 1992). Previous studies have revealed that Be 59 consists of many

PMS stars having age around 2 Myr (Pandey et al. 2008). Be 59 was first studied photographically by Blanco & Williams (1959). They concluded that stars of spectral types O7 to B5 are still surrounded by a part of the parent molecular cloud. A multiwavelength study on Be 59 was presented by Pandey et al. (2008, hereafter P08). They found that this cluster is located at a distance of 1.0 kpc and having a variable extinction of $E(B - V) = 1.4-1.8$ mag. They also found that around 32% of the $H\alpha$ emission stars in Be 59 exhibit NIR excess indicating that they still have their inner disk. During a campaign of photometric monitoring, Ma-jass et al. (2008) presented the nature of the three eclipsing systems (BD+66 $^{\circ}$ 1673, 2MASS 00104558+6127556 and 2MSASS 19064659+4401458) in the field of Be 59 using BV photometry and spectroscopic observations. From the above studies it is clear that Be 59 contains high, intermediate and low mass PMS stars.

PMS objects are, in general, classified into T Tauri stars (TTs) and Herbig Ae/Be stars. The TTs are newly formed low-mass stars ($\lesssim 3M_{\odot}$) which are contracting towards the MS (Herbig 1977), while stars of intermediate mass ($\gtrsim 3-10 M_{\odot}$) are known as Herbig Ae/Be stars (Herbig 1960; Finkenzeller & Mundt 1984; Strom et al. 1972). Herbig Ae/Be stars are either contracting towards MS or they have reached the MS. The TTs can be classified further as Weak line

* E-mail: sneh@aries.res.in

TTSs (WTTSs) and Classical TTSs (CTTSs) on the basis of the strength of the H α emission lines (Strom et al. 1989). The strength of the emission line is measured by its equivalent width (EW). The WTTSs exhibit a weak, narrow H α (EW $\leq 10\text{\AA}$) in emission with no or little infrared excess, while CTTSs generally display strong H α emission line (EW $> 10\text{\AA}$), large ultraviolet and infrared excess. The large H α emission (EW $> 10\text{\AA}$) is believed to be a result of the increased mass accretion onto the star (e.g. Cabrit et al. 1990; Calvet & Hartmann 1992). It is found that PMS stars show strong variability both in photometric and spectroscopic (van den Ancker et al. 1998; Catala et al. 1999) observations. This could be due to the presence of circumstellar obscuration and spots present on the photosphere. In fact variability is a defining characteristics of TTSs (Herbst et al. 1994; Scholz et al. 2009 and references therein). Both WTTSs and CTTSs show variation in their brightness. These variations are found to occur at all wavelengths, from X-ray to infrared. Variability time scale of TTSs ranges from few minutes to years (Appenzeller & Mundt 1989). The photometric variations are believed to originate from several mechanisms like circumstellar gas and dust (remnant of parent molecular cloud), accretion and magnetic field (Herbst et al. 1994). The variations in the brightness of TTSs are most probably due to the presence of spots (cool or hot) at stellar surface and circumstellar disk.

The cool spots on the surface of the stars are produced by the emergence of stellar magnetic fields on the photosphere, and is thus an indicator of magnetic activity. As these spots are present on the photosphere, they rotate with the star. If these spots are symmetrically distributed over the photosphere, periodic variations are seen in the light curves of the stars. Spot configurations remain constant over time-scales of several days, but undergo changes on time-scales of weeks (Hussain 2002). The cool spots on the photosphere of star are responsible for brightness variation in WTTSs, and these objects are found to be fast rotators as they have either thin or no circumstellar disk. Therefore the variability in these objects may be mainly due to the brightness variations on the photosphere modulated by the stellar rotation (Messina et al. 2010).

The hot spots on the surface of young stars are supposed to be formed on the surface by infalling gas and are thus a direct consequence of accretion (Lynden-Bell & Pringle 1974; Koenigl 1991; Shu et al. 1994). Irregular or non periodic variations are produced because of changes in the accretion rate. The time scales of varying brightness range from hours to years. The hot spots cover a smaller fraction of the stellar surface but higher temperature causes larger brightness variations (Carpenter et al. 2001). Thus, accreting CTTSs which are surrounded by circumstellar accretion disk and possess hot spots produced by accreting material from disk on to the star show complex behaviour in their optical and near infrared (NIR) light curves (Scholz et al. 2009).

The Herbig Ae/Be stars also show variability as they move across the instability region in the Hertzsprung-Russell (HR) diagram on their way to the MS. The right combination of mass, temperature and luminosity of these stars make them to pulsate. Several PMS pulsators have been detected until now (Breger 1972; Kurtz & Marang 1995; Marconi et al. 2000; Donati et al. 1997; Zwintz et al. 2005, 2009; Zwintz & Weiss 2006). Catala (2003) presented detailed review on

Table 1. Log of optical photometric CCD observations. ‘Exp.’ and ‘n’ refer to exposure time and number of frames respectively.

date	Object	V (n \times Exp.)	I (n \times Exp.)
21 Dec 2006	Be 59	3 \times 300s, 700s, 700s, 500s	4 \times 300
22 Dec 2006	Be 59	5 \times 700s	-
23 Dec 2006	Be 59	2 \times 700s	-
24 Dec 2006	Be 59	2 \times 700s	3 \times 300s
24 Dec 2006	SA 98	3 \times 200s	3 \times 200s
25 Dec 2006	Be 59	1 \times 700s	-
05 Dec 2007	Be 59	43 \times 50s	-
25 Oct 2008	Be 59	58 \times 50s	-
29 Oct 2008	Be 59	3 \times 50s	-
21 Nov 2008	Be 59	3 \times 50s	-
11 Oct 2009	Be 59	60 \times 300s	-
12 Oct 2009	Be 59	3 \times 300s	-
13 Oct 2009	Be 59	2 \times 300s	-
14 Oct 2009	Be 59	2 \times 300s	-
15 Oct 2009	Be 59	2 \times 300s	-
27 Oct 2010	Be 59	58 \times 200s	-
28 Oct 2010	Be 59	3 \times 200s	-
30 Oct 2010	Be 59	2 \times 200s	-
31 Oct 2010	Be 59	2 \times 200s	-

the PMS pulsations and expected that PMS stars could pulsate as δ Scuti stars, however it is necessary to confirm their PMS nature because these stars are found above the MS where it is very difficult to say whether they are PMS or post MS stars. But in cluster environment where the age of the cluster is constrained well, the stars found towards the cluster region could be PMS stars.

A search of photometric variables in young open cluster Be 59, which is found to have a rich population of PMS stars with a large mass range could give us a better insight of the variability time-scales, the amplitude of brightness variation etc. With this aim, we observed the cluster Be 59 at different epochs from 2006 to 2010. The paper is organised in the following manner. In Section 2, we describe the observations and data reduction techniques. We discuss membership of variable stars on the basis of photometric observations in Section 3. In Section 4, we determine periods of variable stars. We discuss variability characteristics as well as period and amplitude distribution of variable stars in Section 5, while in Section 6 we conclude our studies.

2 OBSERVATIONS AND DATA REDUCTION

Our observing campaign of Be 59 region covers 18 nights from 2006, December 21 to 2010, October 31. Fig. 1 shows the observed field of Be 59. The observations in V band were obtained using 2k \times 2k CCD camera attached to the 104-cm ARIES telescope. As each pixel covers 0.38 arcsec over sky, the field of view is ≈ 13 arcmin on each side. On each night, at least two frames of target field in V band were secured to cover long period variables. The observations of Be 59 consist of total 257 CCD images. In addition, bias and twilight frames were also taken on each night. In order to improve the signal to noise ratio the observations were taken in 2 \times 2 pixel binning mode. Log of the observations is given in Table 1. The preprocessing of the CCD images was

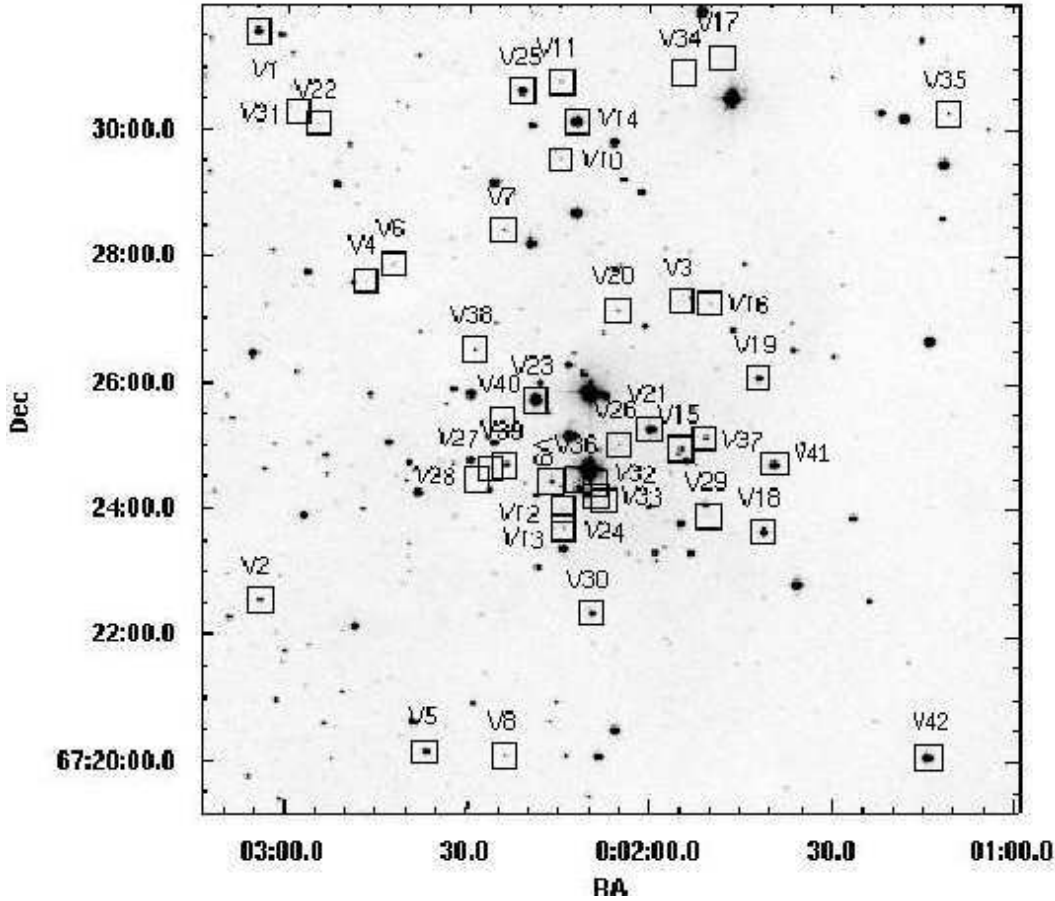


Figure 1. The observed CCD image of Be 59 cluster region. The squares show the location of candidate variables identified in the present work.

done by IRAF which includes bias subtraction, flat fielding and cosmic ray removal. The instrumental magnitude of each star was obtained by DAOPHOT software package given by Stetson (1987). To get the magnitude of each star both the aperture and PSF photometry have been done because the PSF photometry yields better results in crowded region. The standardisation of the observations was done by observing the standard field SA 98 (Landolt 1992). Instrumental magnitudes were converted to standard magnitudes using the following transformations equations

$$v = V + (4.448 \pm 0.004) - (0.037 \pm 0.006)(V - I) + 0.15 * Q$$

$$i = I + (4.767 \pm 0.008) - (0.04 \pm 0.005)(V - I) + 0.05 * Q$$

where v and i are the instrumental magnitudes and Q is the airmass.

2.1 Comparison with Previous Photometry

A comparison of the present photometry with that of P08 yields 342 common stars. Fig. 2 plots difference Δ (present data–literature data) as a function of V magnitude. The comparison indicates a decreasing trend in ΔV values. The ΔV is ≈ -0.13 mag upto $V \approx 14$ mag which decreases to \approx

-0.08 mag upto $V \approx 18$ mag. Whereas present $(V - I)$ colours are comparable to those given by P08.

2.2 Identification of Variables

The DAOMATCH (Stetson 1992) routine of DAOPHOT was used to find the translation, rotation and scaling solutions between different photometry files, whereas DAOMASTER (Stetson 1992) matches the point sources. In order to remove frame-to-frame flux variation of stars due to airmass and exposure time, we used DAOMASTER programme to get the corrected magnitude. This task makes the mean flux level of each frame equal to the reference frame by an additive constant. Present observations have 257 frames and each frame corresponds to one photometry file. DAOMASTER cross identified 472 stars in different photometry files and listed their corrected magnitudes in .cor file, which was used for subsequent tasks. The mean value of the magnitude and square root of the variance (RMS) of the data were estimated using the observations of each star. The RMS as a function of instrumental V magnitude (V_{inst}) is shown in Fig. 3, which indicates that the majority of the stars follow an expected trend i.e., S/N ratio decreases as stars become fainter. However, a few stars do not follow the normal trend and exhibit relatively large scatter. These could be either due to the large photometric errors or due to the variable

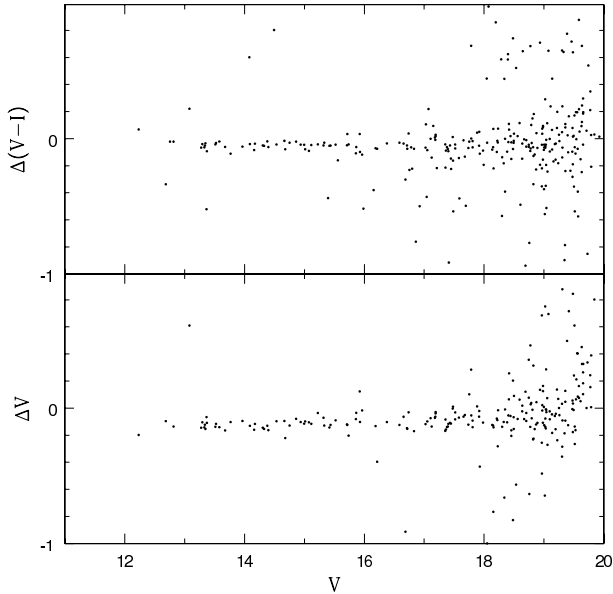


Figure 2. Comparison of the present photometry and photometry given by Pandey et al. (2008).

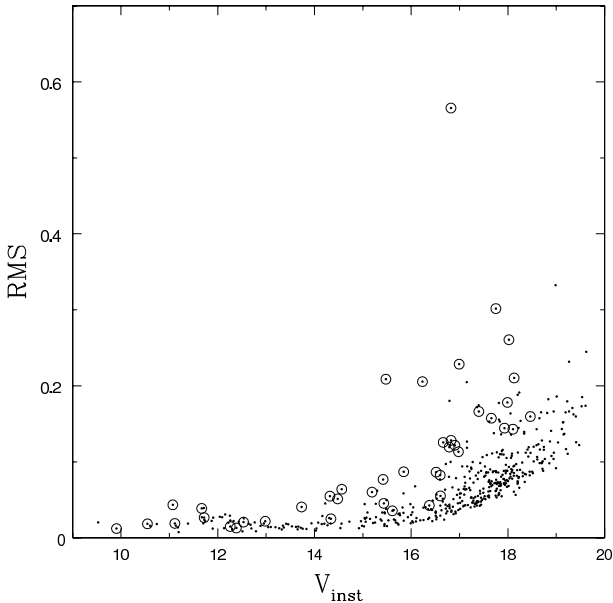


Figure 3. RMS for each star as a function of brightness. Open circles represent candidate variables identified in the present work. Some stars showing large RMS are not considered variable stars as they are located near the edge of the CCD.

nature of the stars. We considered a star as variable if its RMS is greater than 3 times of the mean RMS of that bin. Forty five candidate variables were thus identified on the basis of above mentioned criterion. On the basis of a careful inspection of light curves and the location of the sources on the CCD frames, we selected a sample of 37 stars to study their nature. A few stars were rejected as they were lying near the edge at the CCD. The mentioned technique, however, could not detect low amplitude variables and 5 variables namely V14, V18, V21, V23 and V19 were detected manually by inspecting their light curves. Thus we have a

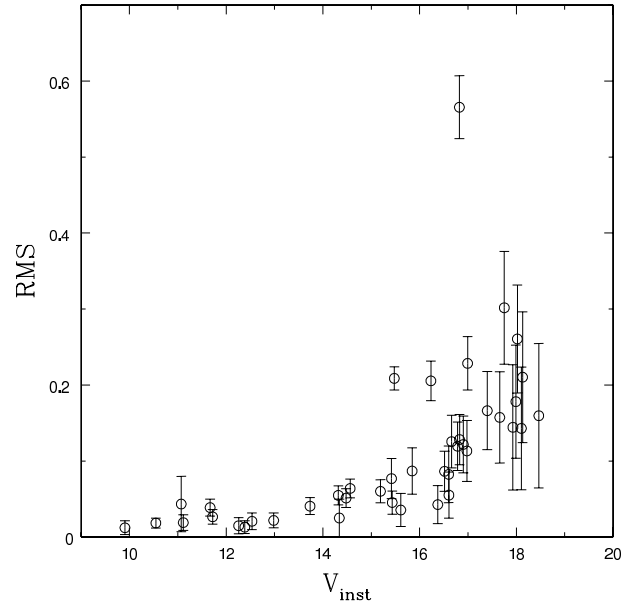


Figure 4. The RMS along with mean photometric errors of the detected variable stars as a function of instrumental magnitude.

sample of 42 variables. Their identification numbers, coordinates and photometric data are given in Table 2. The RMS along with mean photometric errors of detected variables as a function of instrumental magnitude are shown in Fig. 4. The photometric error is found to be ~ 0.010 mag at $V_{inst} \leq 14$ mag, whereas the value of photometric error increases to ~ 0.08 mag at ~ 18 mag.

Out of three variable stars reported by Majaess et al. (2008), only one variable star (BD+66°1673) is located in the present observed field of Be 59. Unfortunately, this star was saturated in our observations.

In order to find out the possible causes of photometric variations in the identified variable stars in the region of Be 59, it is important to ascertain their membership. In the absence of spectroscopic observations, we established photometric membership on the basis of $(V, V - I)$ colour-magnitude and $(J - H, H - K)$ colour-colour diagram in next Section.

3 CLUSTER MEMBERSHIP

The colour-magnitude diagram (CMD) of the cluster region clearly reveals contamination due to field star population (cf. figure 7 by P08). P08 found that the cluster is located at a distance of 1.00 ± 0.05 kpc and has a differential reddening $E(B - V) = 1.4 - 1.8$ mag. They also identified a foreground field star population at a distance of ~ 470 pc with a $E(B - V) = 0.40$ mag (cf. figure 4 of P08). Therefore, the sample of identified variables may be contaminated by foreground population. We have used V , $(V - I)$ CMD and NIR $J - H$, $H - K$ colour-colour diagram to find out the association of the identified variables with the cluster Be 59.

Table 2. Basic parameters of 42 variables in open cluster Be 59. $H\alpha$ sources are taken from Pandey et al. (2008).

ID	α_{2000}	δ_{2000}	V mag	$(V - I)$ mag	J mag	H mag	K mag	Age Myrs	Mass M_{\odot}	Amp. mag	Period day	Object Type
V1	0.77192	67.52431	13.984	1.449	11.519	11.197	11.045	-	-	0.023	0.225	FGMS ¹
V2	0.76846	67.37411	16.154	2.424	12.038	11.318	11.083	5.00	2.50	0.039	0.539	PMS
V3	0.47883	67.45319	19.724	3.241	15.612	13.799	12.535	3.50	0.80	0.855	89.800	PMS, IR excess, CTTS
V4	0.69671	67.45858	19.082	3.396	13.420	12.128	11.427	1.00	0.65	0.272	0.652	PMS, IR excess, CTTS
V5	0.65492	67.33436	15.386	1.315	13.118	12.627	12.540	-	-	0.041	0.508	FGMS
V6	0.67825	67.46291	18.332	3.033	13.115	12.103	11.725	1.50	1.10	0.066	0.527	PMS
V7	0.60192	67.47219	17.366	3.037	12.066	10.895	10.266	0.50	1.10	0.270	6.586	PMS, $H\alpha$, IR excess, CTTS
V8	0.60004	67.33353	18.045	2.763	13.244	12.463	12.084	4.00	1.85	0.067	1.775	PMS
V9	0.56908	67.40567	15.925	2.832	11.047	10.147	9.764	0.15	2.50	0.030	0.974	PMS
V10	0.56275	67.49089	19.024	3.036	13.175	11.958	11.051	4.00	1.10	1.122	1.102,58.753	PMS, $H\alpha$, IR excess, CTTS
V11	0.56254	67.51144	18.402	2.991	13.141	12.157	11.748	2.00	1.25	0.122	0.441	PMS
V12	0.56121	67.39845	18.753	3.339	12.968	11.917	11.522	0.80	0.70	0.273	5.671	PMS
V13	0.56029	67.39361	17.931	2.994	12.486	11.261	10.486	1.00	1.25	0.290	1.212	PMS, IR excess, CTTS
V14	0.55221	67.50259	12.427	0.947	10.693	10.340	10.206	-	-	0.016	0.158	FGMS
V15	0.47992	67.41450	16.210	2.026	12.733	11.672	10.704	20.00	2.00	0.215	10.317	PMS, IR excess, CTTS
V16	0.45971	67.45303	18.673	3.167	13.238	12.083	11.605	1.00	0.90	0.125	1.137	PMS
V17	0.45217	67.51797	19.933	3.689	13.794	12.533	11.986	1.00	0.45	0.354	0.688	PMS, IR excess, CTTS
V18	0.42346	67.39261	13.263	0.884	11.784	11.390	11.331	-	-	0.017	0.301	FGMS
V19	0.42633	67.43320	14.665	2.420	10.559	9.844	9.496	1.50	3.50	0.022,0.014	0.109,0.101,0.096	PMS, Herbig Ae/Be
V20	0.52329	67.45094	17.483	2.816	12.653	11.711	11.309	1.50	2.00	0.095	0.491	PMS
V21	0.50100	67.41972	12.675	1.258	10.249	9.881	9.731	-	-	0.048	0.338	FGMS
V22	0.72962	67.49997	18.887	3.531	12.952	11.919	11.558	0.50	0.55	0.111	0.646	PMS
V23	0.58017	67.42725	11.806	2.657	7.179	6.552	6.214	0.10	-	0.027	0.217	PMS
V24	0.53228	67.40089	19.595	3.401	14.298	13.281	12.877	1.50	0.65	0.152	0.828	PMS
V25	0.58971	67.50886	14.073	1.560	11.500	11.175	10.933	-	-	0.200	0.488	FGMS
V26	0.52221	67.41542	18.162	2.938	13.071	12.089	11.723	2.00	1.40	0.083	0.623	PMS
V27	0.60962	67.40936	18.598	3.158	12.919	11.864	11.457	1.00	0.90	0.085	1.925	PMS
V28	0.62008	67.40633	20.239	3.555	13.780	12.533	11.793	1.50	0.50	0.356	9.735	PMS, IR excess, CTTS
V29	0.46017	67.39688	20.089	2.392	15.900	14.416	14.450	-	-	0.300	1.158	FGMS
V30	0.54121	67.37103	14.151	1.270	12.032	11.438	11.337	-	-	0.025	0.472	FGMS
V31	0.74446	67.50539	19.944	3.485	14.025	12.992	-	1.50	0.60	0.221	0.516	PMS, IR excess, CTTS
V32	0.53858	67.40721	18.703	4.126	-	-	-	0.10	0.30	0.203	0.313	PMS
V33	0.53746	67.40406	18.423	3.308	13.256	12.296	11.939	0.80	0.70	0.110	1.014	PMS
V34	0.47832	67.51580	19.466	3.209	13.869	12.662	11.975	1.50	0.70	0.315	0.423	PMS, IR excess, CTTS
V35	0.29528	67.50493	17.331	2.541	13.627	13.246	12.994	-	-	0.030	0.460	FGMS
V36	0.55012	67.40846	17.190	3.229	12.208	11.249	10.884	0.30	0.90	0.072	0.514	PMS
V37	0.46255	67.41744	16.738	2.422	12.575	11.718	11.400	10.00	2.00	0.044	0.796	PMS
V38	0.62147	67.44061	17.024	2.783	12.279	11.330	10.987	1.00	2.50	0.064	1.020	PMS
V39	0.59997	67.41019	15.961	2.220	11.992	11.169	10.896	10.00	2.00	0.025	0.325	PMS
V40	0.60189	67.42397	19.467	3.357	14.388	14.141	13.061	3.00	0.85	0.175	1.757	PMS
V41	0.41556	67.41031	13.337	1.221	11.328	10.925	10.793	-	-	0.029	0.787	FGMS
V42	0.31053	67.33290	12.745	1.134	10.931	10.490	10.395	-	-	0.021	0.335	FGMS

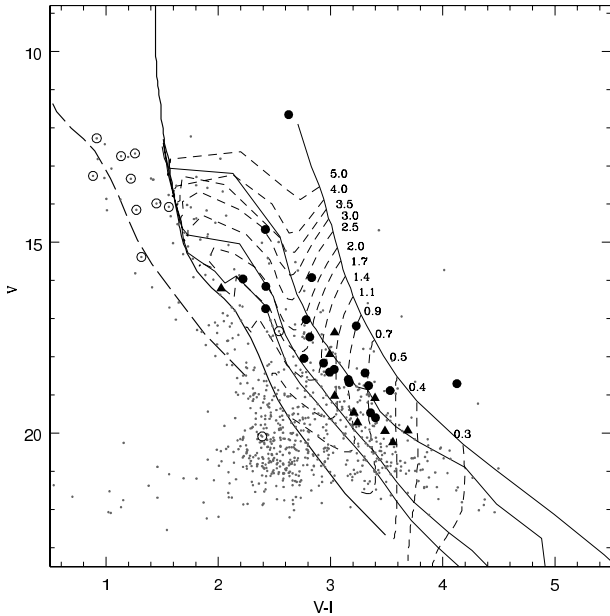
¹:foreground MS


Figure 5. $V, V - I$ colour-magnitude diagram of Be 59. The ZAMS by Girardi et al. (2002) and PMS isochrones for 0.1, 1, 5, 10 Myrs by Siess et al. (2000) are also shown. The dashed curves show PMS evolutionary tracks for stars of different masses. The isochrones and evolutionary tracks are corrected for the cluster distance and $E(B - V) = 1.45$ mag. The filled circles and triangles represent probable WTTs and CTTSs respectively (cf. section 3.2). The thick dashed is ZAMS by Girardi et al. (2002) corrected for a distance of 470 pc and reddening $E(B - V) = 0.40$ mag. The open circles represent foreground stars.

3.1 $V, (V - I)$ Colour-Magnitude Diagram

Fig. 5 displays $V, (V - I)$ CMD for the stars observed in the cluster. The identified variables are marked by triangles (CTTSs) and filled circles (WTTs) (cf. section 3.2). The zero-age main-sequence (ZAMS) by Girardi et al. (2002) corrected for the distance of 1.0 kpc and $E(B - V) = 1.45$ mag is shown by thick continuous line. The pre-main-sequence (PMS) isochrones for 0.1, 1, 5 and 10 Myrs by Siess et al. (2000) have also been overplotted. The ZAMS corrected for a distance of 470 pc and $E(B - V) = 0.40$ mag for the foreground population is shown by thick dashed curve. Fig. 5. reveals that the stars V1, V5, V14, V18, V21, V25, V29, V30, V35, V41 and V42 (shown with open circles) follow the ZAMS for field stars, hence could be MS foreground population. It is worthwhile to point that majority of the field stars (10 out of 11) are located outside the core (1.4 arcmin, P08) of the cluster.

In order to determine the ages and masses of the probable PMS variable stars we have used PMS isochrones and evolutionary tracks by Siess et al. (2000), respectively. Majority of the probable PMS cluster members have masses in the range $0.3 \lesssim M/M_{\odot} \lesssim 3.5$ and ages in the range $1 \lesssim \text{age} \lesssim 5$ Myrs. This indicates that the young stellar objects associated with the cluster could be TTSs. Star V23 is the brightest variable in the sample and lies near 0.1 Myr PMS isochrone.

3.2 NIR Colour-Colour Diagram

The NIR colour-colour diagram (CCD) can be used to distinguish the CTTSs and WTTs. Fig. 6 shows NIR CCD for the

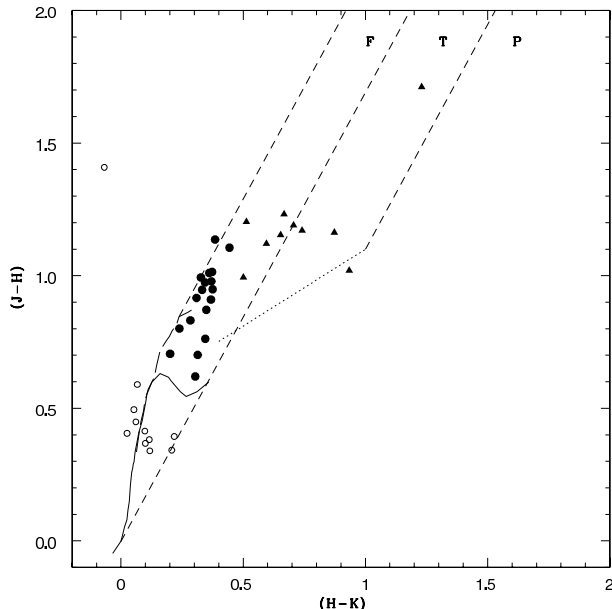


Figure 6. $(J - H, H - K)$ colour-colour diagram for stars lying in the 13×13 arcmin² field of Be 59. JHK data have been taken from 2MASS catalogue. The symbols are same as in Fig. 5. The sequences for dwarfs (solid) and giants (long dashed) are from Bessel & Brett (1988). The dotted line represents the intrinsic locus of CTTSs (Meyer et al. 1997). Dashed lines represent the reddening vectors (Cohen et al. 1981).

identified variables. The NIR data have been taken from the 2MASS Point Source Catalogues (PSC; Cutri et al. 2003). The 2MASS counterpart of the variables were searched using a match value of 3 arcsec. Of the 42 detected variables, we found 2MASS counterparts for 41 stars (30 cluster members and 11 foreground MS stars). The 2MASS counterpart for V32 star could not be found. It is the reddest variable star in the sample and lying above 0.1 Myr PMS isochrone in $V, (V - I)$ CMD. However, on the basis of the location of this star on $V, (V - I)$ CMD, we have considered V32 as a PMS object. The 2MASS magnitudes and colours were transformed to the CIT system using the relations given on the 2MASS website. The solid and long dashed lines represent unreddened MS and giant branch (Bessell & Brett 1988), respectively. The dotted line indicates intrinsic locus of CTTSs (Meyer et al. 1997). The parallel dashed lines are the reddening vectors drawn from the tip (spectral type M4) of the giant branch (‘upper reddening line’), from the base (spectral type A0) of the main-sequence branch (‘middle reddening line’) and from the tip of the intrinsic CTTS line (‘lower reddening line’). The extinction ratios $A_J/A_V = 0.265$, $A_H/A_V = 0.155$ and $A_K/A_V = 0.090$ have been adopted from Cohen et al. (1981). We classified the sources into three regions in the NIR CCD (cf. Ojha et al. 2004a). The ‘F’ sources are those that are located between the upper and middle reddening lines and are considered to be either field stars (main-sequence stars, giants) or Class III and Class II sources with small NIR excesses. The identification of Class II sources having a small amount of NIR excess is difficult on the basis of $(J - H, H - K)$ CCD. However, recent studies, where Class II sources were identified on the basis of mid-IR observations through Spitzer telescope,

manifest that these Class II objects lie in ‘F’ region near the middle reddening vector (e.g. Chauhan et al. 2011). The ‘T’ sources are those that are located between the middle and lower reddening lines. These sources are considered to be mostly CTTSs (Class II objects). ‘P’ sources are those that are located in the region redward of the T region and are most likely Class I objects (protostar-like objects; Ojha et al. 2004b).

Majority of the stars lying in the ‘F’ region are considered as Class III stars/WTTs and are shown by filled circles. However, there seems segregation of sources between $(J - H) \gtrsim 1.0$ mag and $(H - K) \gtrsim 0.50$ mag in $(J - H, H - K)$ colour-colour diagram. As discussed above that Class II sources with small amount of NIR excess could be found in ‘F’ region near the middle reddening vector. The stars having $(J - H) \gtrsim 1.0$ mag and $(H - K) \gtrsim 0.50$ mag are considered CTTS and these are shown by filled triangles. The foreground MS stars as identified from $V, V - I$ CMD are distributed around the ZAMS and shown by open circles. The nature of the identified variables is mentioned in the Table 2.

The membership of the variable stars is determined on the basis of their location in $(V, V - I)$ CMD and NIR CCD. However, spectroscopic follow up of these objects is needed to confirm their nature.

4 PERIOD DETERMINATION

We used the Lomb-Scargle (LS) periodogram (Lomb 1976; Scargle 1982) to determine the most likely period of a variable star. The LS method is useful for finding significant periodicities even with unevenly sampled data. We used the algorithm publicly available at the Starlink² software database, and verified the periods further with the software period04³ (Lenz & Breger 2005). The software period04 provides the frequency and semi-amplitude of the variability in a light curve. Periods derived from the LS method and Period04 generally matched well. In order to further verify the period estimates we also used periodogram analysis available online⁴. For any star showing a spurious period, we visually inspected the phased light curve for that particular period. The phased light curves for CTTSs, WTTs and field stars are shown in Figs. 7, 8 and 9, and 10 respectively. Figs. 7, 8, 9 and 10 plot the mean of differential magnitudes in 0.04 phase bin as a function of phase. The error bars represent the σ of the mean. In subsequent section we discuss the variability characteristics of individual variable star.

5 VARIABILITY CHARACTERISTICS

5.1 Non Periodic Variables

Light curve of one WTTs variable named V38 displayed in Fig. 9 does not show periodic variability. This star could be either irregular variable or the period estimated in the present work could be in error.

² <http://www.starlink.uk>

³ <http://www.univie.ac.at/tops/Period04>

⁴ <http://nsted.ipac.caltech.edu/periodogram/cgi-bin/Periodogram/nph-simpleupload>

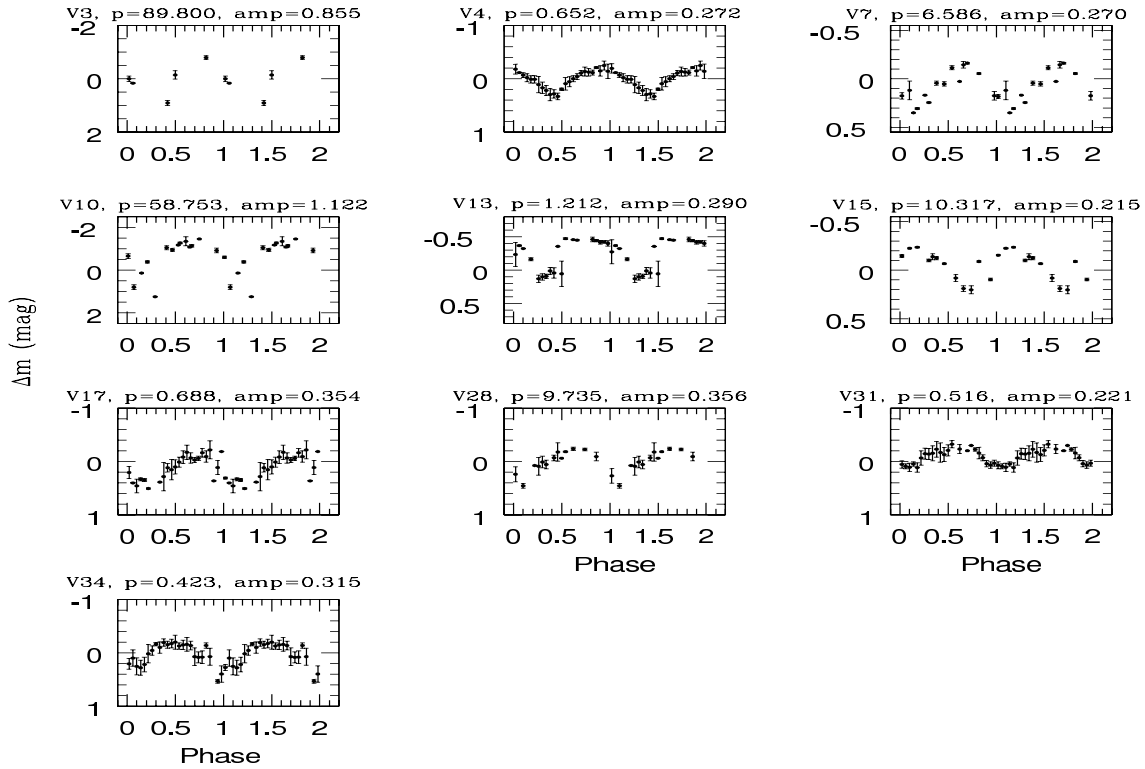


Figure 7. The phased light curves of probable CTTSs candidate variables identified in Be 59.

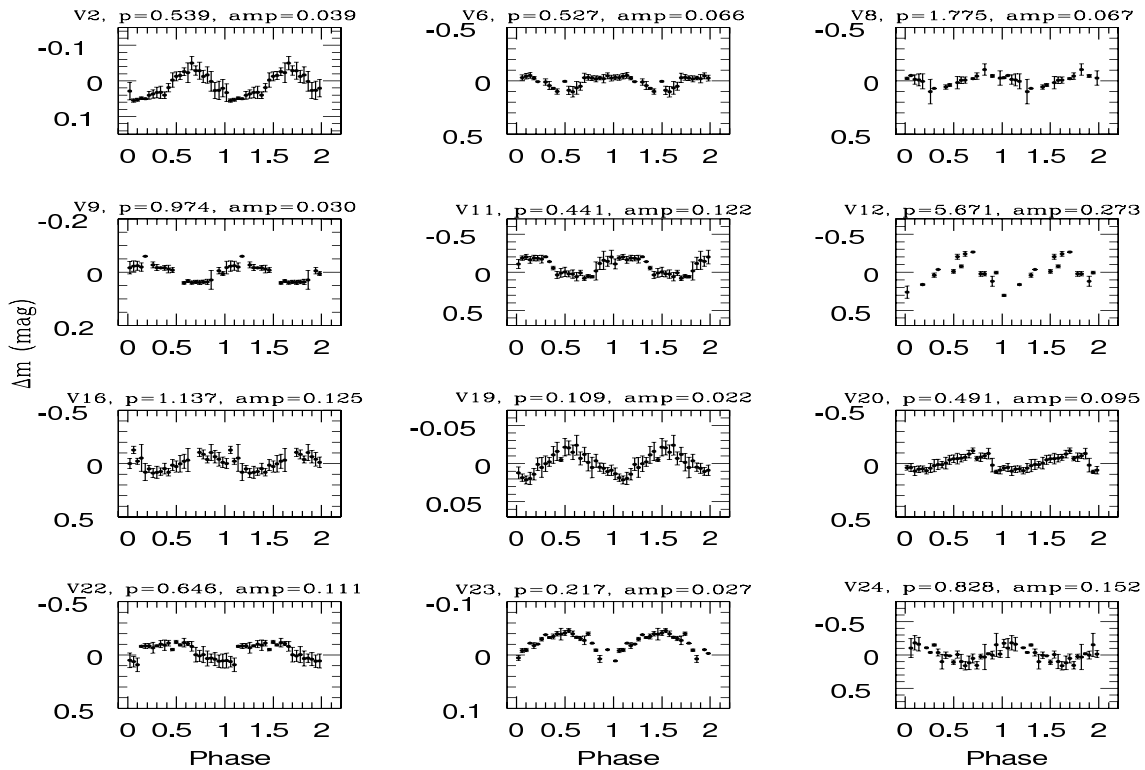


Figure 8. The phased light curves of probable WTTSs candidate variables identified in Be 59.

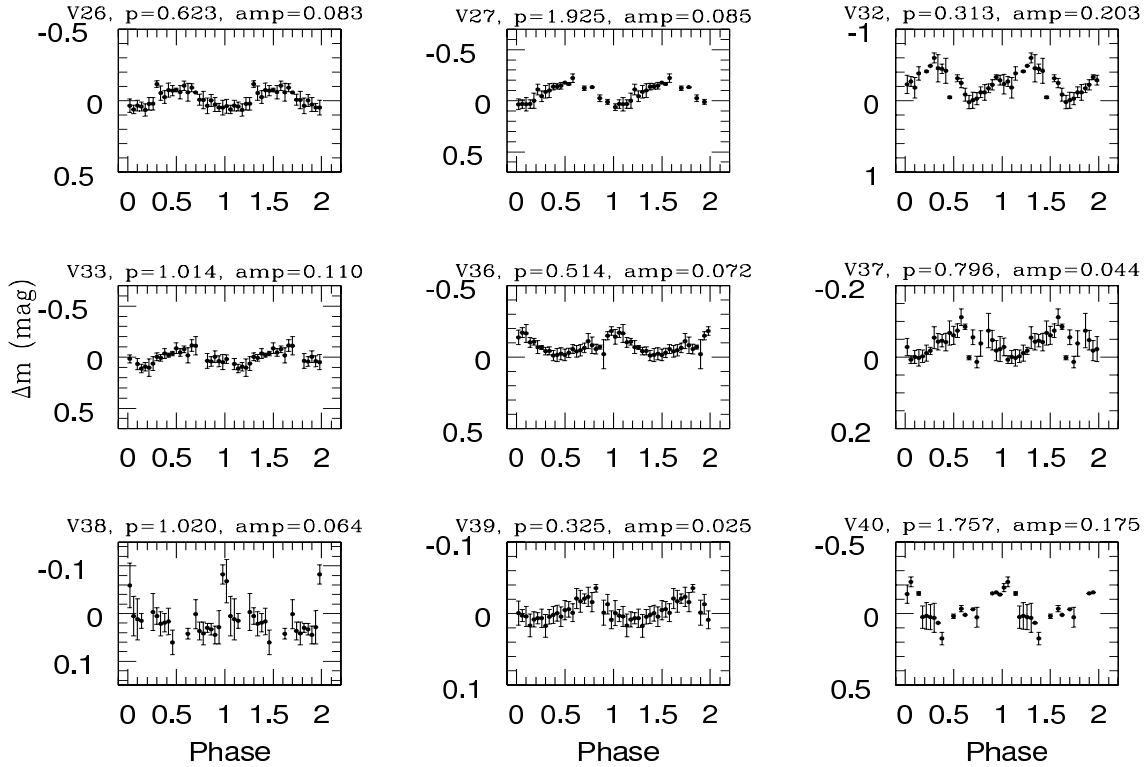


Figure 9. Same as Fig. 8.

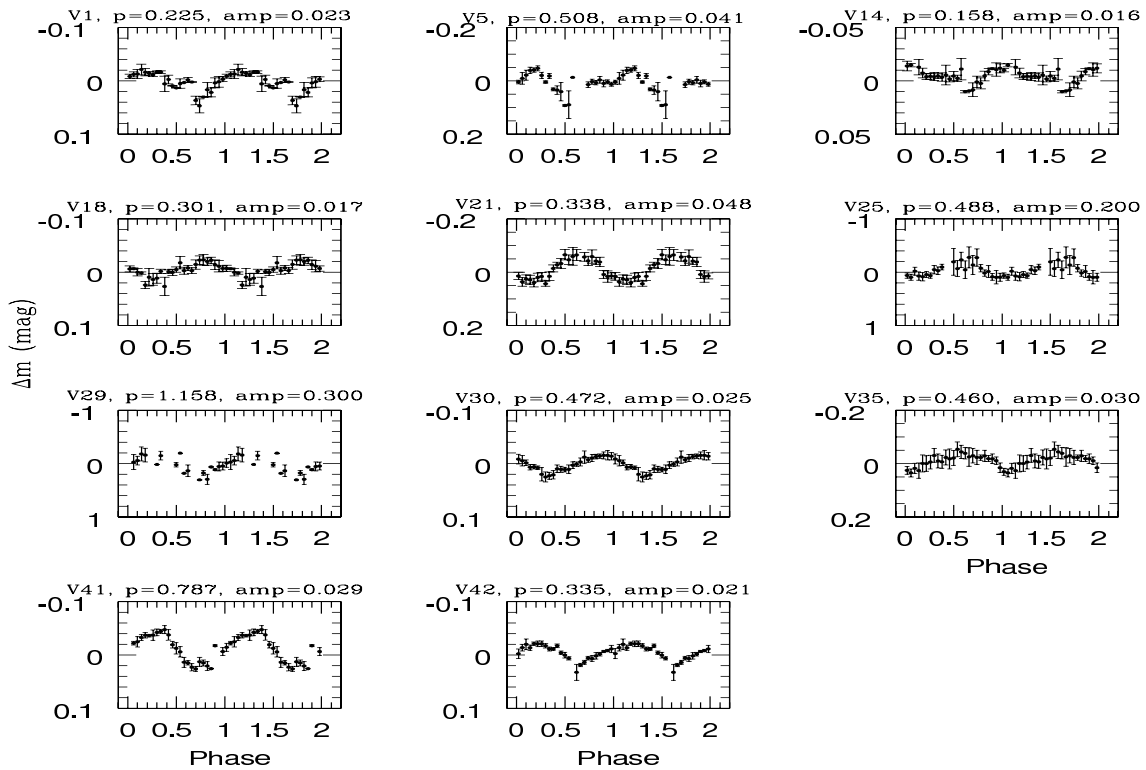


Figure 10. The phased light curves of foreground MS variables.

5.2 Periodic Variables

The short term periodic variations ($2 \sim 10$ days) in TTSs are believed to occur due to the axial rotation of a star with an inhomogeneous surface, having either hot or cool spots (Herbst et al. 1987, 1994). Herbst et al. (1994) identified three types of TT variables based on their variability timescales ranging from a day to weeks. Type I variability, most often seen in WTTSs, is characterized by smaller stellar flux variations (a few times of 0.1 mag) and results from the rotation of a cool spotted photosphere. Type II variations have larger brightness variations (up to ~ 2 mag), most often irregular but sometime periodic, are associated with short-lived accretion related hot spots at the stellar surface of CTTSs. The rare type III variations are characterized by luminosity dips lasting from a few days upto several months, which presumably result from circumstellar dust obscuration. The sample of TTSs in the cluster Be 59 indicates that $\sim 90\%$ TTSs have periods less than 15 days. The estimated periods of 8 CTTSs vary in the range of 0.652 day to 10.317 day, however stars V3 and V10 have significantly larger periods (89.8 day and 58.7 day respectively). The period estimates for WTTSs vary from 0.109 day to 5.671 day, however $\sim 95\%$ WTTSs have periods ≤ 2 day. The shorter periods in the case of WTTSs could be explained as most of the stars at this age might have unlocked from their disks while contracting towards MS. They spin up because of decreasing radii in order to conserve their angular momentum (Strom et al. 1989; Skrutskie et al. 1990; Haisch et al. 2001; Bouvier et al. 1994; Herbst & Mundt 2005; Lamm et al. 2005; Kundurthy et al. 2006). But Nordhagen et al. (2006) have different view and suggest that environment also plays a crucial role in establishing the rotation periods besides age and mass. The presence of ‘O’ type stars in the vicinity would speed up the process of the dispersal of the circumstellar disks causing the stars to spin up at a much younger age.

The amplitude of WTTSs ranges from 0.022 to 0.273 mag. The amplitude in the case of CTTSs has a range of 0.215 to 1.122 mag. The present results regarding amplitudes are in agreement with Grankin et al. (2008 for WTTSs) and Grankin et al. (2007 for CTTSs). The brightness of CTTSs is found to vary with larger amplitude in comparison to the WTTSs. The large amplitude in the case of CTTSs indicates presence of the hot spots on their surfaces. The smaller amplitude in the case of WTTSs suggests that these PMS stars might be in the process of dissipation of their circumstellar disk.

The star V3, a probable CTTS, seems to be an interesting object. It has relatively high excess ($H - K = 1.23$) and shows relatively high extinction (cf. Fig. 6). It has a period of 89.80 days with amplitude variation of 1.0 mag and its mass is estimated to be $\sim 0.9 M_{\odot}$. The relatively high extinction of this object could be due to the presence of the circumstellar disk. Edwards et al. (1993) found that the stars which showed the evidence of circumstellar disks, inferred from their ($H - K$) colours, are slow rotators in comparison to those that lacked circumstellar disks. Relatively high extinction and longer period of V3 support this argument. This star may belong to type III as classified by Herbst et al. (1994), where relatively larger luminosity dips

for longer period are expected due to circumstellar dust obscuration.

The H α emission star V10, classified as CTTS, also seems to be an interesting object. A careful inspection of night to night observations of this star reveals amplitude variation. Its 2006 observations show that the brightness of this star was varying with larger amplitude (1.122 mag) and period 1.102 day. From 2007 and onwards, it shows consistent brightness variation with amplitude of ~ 0.20 mag and period of 1.102 day. Whereas, the whole data set yield a period of 58.753 day.

Star V19 ($V = 14.665$ mag) could be a PMS pulsating star as suggested by its variability characteristics like period, amplitude and the shape of light curve. The period and amplitude of star V19 vary over time. Its period on 11 October 2009 and 27 October 2010 is found to be 0.101 day and 0.096 day, respectively, whereas its amplitude varied from 0.022 to 0.014 mag on respective dates. Considering all the observations of this star its period comes out to be 0.109 day. Star V19 might be a δ Scuti type variable star.

An early type star V23 (brightest star in the present sample), considered to be a member of the cluster, might be a pulsating star. Its period (0.217 day) and amplitude (0.027 mag) are very much similar to the B-type pulsating stars.

Star V21, lying just below the MS, could be a cluster member. The period, amplitude and the shape of light curve of V21 suggest that it might be a pulsating star. The spectroscopic observations of star V21 was made by Majaess et al. (2008). They considered it to be a member of the cluster Be 59 and found it to be a B-type star.

The field variables have period < 1.16 days and amplitude < 0.30 mag.

5.3 Period and Amplitude Distribution

In order to study the correlation between stellar activity and mass/age, we plot rotation period as a function of mass/age in Fig. 11. The rotation periods of TTSs associated with the cluster Be 59 do not show any dependency on the mass (Fig. 11 left panel). Fig.11 (right panel) shows two long periodic variables (V3 with $P=89.8$ day and V10 with $P=58.753$ day, cf. Table 2) have ages less than 5 Myrs, which could be interpreted as the rotation is regulated by disk locking at early ages (Jayawardhana et al. 2006, Herbst et al. 2002). The presence of NIR excess in ($H - K$) of V3 and H α emission in case of V10 is probably indicative of disk locking. But it is worth to mention here that large IR excess alone could not indicate ongoing disk-locking because IR excess is the indicator for the presence of circumstellar dust and it is not an indicator for current mass accretion (Lamm et al. 2005).

Fig. 12 (left panel) and Fig. 12 (right panel) show amplitude as function of mass and age, respectively. Fig. 12 (left panel) reveals that the amplitude of TTSs seems to be correlated with the mass of the star in the sense that amplitude decreases with increasing mass of the variables. The largest amplitude is found in the case of V3 (0.855 mag) and V10 (1.122 mag). The star V3 shows significantly higher ($H - K$) excess with relatively larger extinction, whereas star V10 shows H α emission. Thus both the stars manifest presence of disk. The decrease in amplitude could be due to the dispersal of the disk material. If this notion is true, it in-

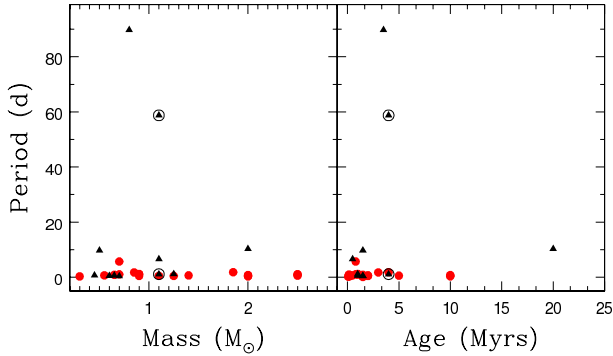


Figure 11. Rotation period as a function of mass and age of CTTs and WTTSs. The symbols are same as in Fig. 5. The encircled triangles represent long and short periods for V10.

icates that the mechanism for disk dispersal operates less efficiently for relatively low mass stars. In fact there is evidence in literature that disk dispersal mechanism depends on the mass of the stars (e.g. Carpenter et al. 2006). But in Fig 12. (right panel), the amplitude variation with ages shows no definite trend, and majority of the sources having the ages within 5 Myrs show the amplitude of variability up to 0.35 mag with two CTTs as exception, which have been discussed earlier.

6 SUMMARY

The paper presents our efforts to search for variable stars in young open cluster Be 59. Using *VI* photometry of a $\sim 13' \times 13'$ field around the cluster we have identified 42 variable stars. The probable members of the cluster are identified using (*V, V - I*) colour-magnitude diagram and (*J - H, H - K*) colour-colour diagram. Out of 42 variables, 31 variable stars are found to be the probable PMS stars associated with the cluster Be 59. The majority of the probable PMS candidate variable stars have ages 1 to 5 Myrs. The masses of probable PMS variable stars range from ~ 0.3 to $\sim 3.5 M_{\odot}$, suggesting that these could be TTSs. The sample of TTSs in the cluster Be 59 indicates that $\sim 90\%$ TTSs have periods less than 15 days. The CTTs have larger amplitudes in comparison to WTTSs. The larger amplitude of CTTs indicates the presence of hot spots on their surface. The smaller amplitude in the case of WTTSs suggests that these PMS stars might be in the process of dissipation of their circumstellar disk. It is found that the amplitude of TTSs decreases with increasing mass of the variable stars. The decrease in amplitude of variability of TTSs could be due to the dispersal of the disk material, indicating that the mechanism for disk dispersal operates less efficiently for relatively low mass stars.

7 ACKNOWLEDGMENTS

Authors are very thankful to the anonymous referee for useful suggestions, which improved the scientific contents of the paper.

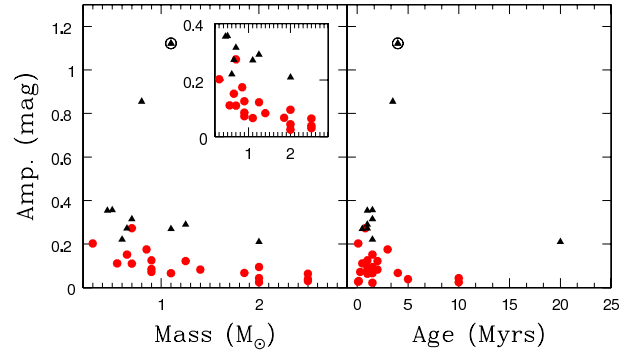


Figure 12. Amplitude as a function of mass and age of CTTs and WTTSs. The symbols are same as in Fig. 5 and Fig. 11. Inset in the left panel shows a magnified view of amplitude variation.

REFERENCES

- [Alves de Oliveira C., Casali M., 2008, *A&A*, 485, 155
- [Appenzeller I., & Mundt R., 1989, *Astron. Astrophys. Rev.* 1, 291
- [Breger M., 1972, *ApJ*, 176, 367
- [Blanco V. M., Williams A. D., 1959, *ApJ*, 130, 482
- [Bessell M. S., Brett J. M., 1988, *PASP*, 100, 1134
- [Bouvier J., Malbet F., Monin J. -L., 1994, *Ap&SS*, 212, 159
- [Cabrit S., Edwards S., Strom S. E., Strom K. M., 1990, *ApJ*, 354, 687
- [Calvet N., Hartmann L., 1992, *ApJ*, 386, 239
- [Carpenter J. M., Hillenbrand L. A., Skrutskie M. F., 2001, *AJ*, 121, 3160
- [Carpenter J. M., Mamajek E. E., Hillenbrand L. A., Meyer M. R., 2006, *ApJ*, 651, 49
- [Catala C., 2003, *Ap&SS*, 284, 53
- [Catala C., Donati J. F., Böhm T., Landstreet J., Henrichs H. F., Unruh Y., Hao J., Collier C. A., Johns-Krull C. M., Kaper L., et al., 1999, *A&A*, 345, 884
- [Cutri R. M., Skrutskie M. F., van Dyk S., et al., 2003, *2MASS All Sky Catalog of point sources*.
- [Cohen J. G., Persson S. E., Elias J. H., Frogel J. A., 1981, *ApJ*, 249, 481
- [Chauhan N., Pandey A. K., Ogura K., Jose J., Ojha D. K., Samal M. R., Mito H., 2011, *MNRAS*, 415, 1202
- [Donati J. -F., Semel M., Carter B. D., Rees D. E., Collier Cameron A., 1997, *MNRAS*, 291, 658
- [Edwards S., Strom S. E., Hartigan P., Strom K. M., Hillenbrand L. A., Herbst W., Attridge J., Merrill K. M., Probst R., Gatley I., 1993, *AJ*, 106, 372
- [Finkenzeller U., Mundt R., 1984, *A&AS*, 55, 109
- [Grankin K. N., Melnikov S. Yu., Bouvier J., Herbst W., Shevchenko V. S., 2007, *A&A*, 461, 183
- [Grankin K. N., Bouvier J., Herbst W., Melnikov S. Y., 2008, *A&A*, 479, 827
- [Girardi L., Bertelli G., Bressan A., Chiosi C., Groenewegen M. A. T., Marigo P., Salasnich B., & Weiss A., 2002, *A&A*, 391, 195
- [Herbst W., Herbst D. K., Grossman E. J., Weinstein D., 1994, *AJ*, 108, 1906
- [Herbst W., Booth J. F., Korett F. L., et al, 1987, *AJ*, 94, 137
- [Herbst W., Mundt R., 2005, *ApJ*, 633, 967

- Herbst W., Bailer-Jones C. A. L., Mundt R., Meisenheimer K., Wackermann R., 2002, *A&A*, 396, 513
- Herbig G. H., 1960, *ApJS*, 4, 337
- Herbig G., 1977, *ApJ*, 214, 747
- Haisch K. E., Lada E. A., Lada C. J. 2001, *ApJ*, 553, L153
- Hussain G. A. J., 2002, *Astron. Nachr.*, 323, 349
- Jayawardhana R., Coffey J., Scholz A., Brandeker A., van Kerkwijk M. H., 2006, *ApJ*, 648, 1206
- Koenigl A., 1991, *ApJ*, 370, 39
- Kurtz D. W., Marang F., 1995, *MNRAS*, 276, 191
- Kundurthy P., Meyer M. R., Robberto M., Beckwith S. V. W., Herbst T., 2006, *AJ*, 132, 2469
- Lamm M. H., Mundt, R., Bailer-Jones C. A. L., Herbst W., 2005, *A&A*, 430, 1005
- Landolt A. U., 1992, *AJ*, 104, 340
- Lenz P., Breger, M., 2005, *Comm. Asteroseismol.*, 146,53
- Lomb N.R., 1976, *ApSS*, 39, 447
- Lynden-Bel D., Pringle J. E., 1974, *MNRAS*, 168, 603
- Majaess D. J., Turner D. G., Lane D. J., Moncrieff K. E., 2008, *JAVSO*, 36, 90
- Marconi M., Ripepi V., Alcalá J. M., Covino E., Palla F., Terranegra L., 2000, *A&A*, 355, L35
- Messina S., Parihar P., Koo J.-R., Kim S.-L., Rey S.-C., Lee C.-U., 2010, *A&A*, 513, 29
- Meyer M. R., Calvet N., Hillenbrand, L. A., 1997, *AJ*, 114, 288
- Nordhagen S., Herbst W., Rhode K. L., Williams E. C., 2006, *AJ*, 132, 1555
- Ojha D. K. et al., 2004a, *ApJ*, 608, 792
- Ojha D. K. et al., 2004b, *ApJ*, 616, 1042
- Pandey A. K., Sharma S., Ogura K., Ojha D. K., Chen W. P., Bhatt B. C., Ghosh S. K., 2008, *MNRAS*, 383, 1241
- Scargle J.D., 1982, *ApJ*, 263, 835
- Scholz A., Eisloffel J., Mundt R., 2009, *MNRAS*, 400, 1548
- Shu F. H., Najita J., Ruden S. P., Lizano S., 1994, *ApJ*, 429, 797
- Siess L., Dufour E., Forestini M., 2000, *A&A*, 358, 593
- Strom K. M., Strom S. E., Edwards S., Cabrit S., Skrutskie, M. F. 1989, *AJ*, 97, 1451
- Strom S. E., Strom K. M., Yost J., et al, 1972, *ApJ*, 173, L65.
- Skrutskie M. F., Dutkevitch D., Strom S. E., Edwards S., Strom K. M., Shure M. A. 1990, *AJ*, 99, 1187
- Stetson P. B., 1987, *PASP*, 99, 191
- Stetson P. B., 1992, *J. R. Astron. Soc. Can.*, 86, 71
- van den Ancker M. E., de Winter D., Tjin A Djie H. R. E., 1998, *A&A*, 330, 145
- Yang J., Fukui Y., 1992, *ApJ*, 386, 618
- Zwintz K., Marconi M., Reegen P., et al. 2005, *MNRAS*, 357, 345
- Zwintz K., Weiss W. W., 2006, *A&A*, 457, 237
- Zwintz K., Hareter M., Kuschnig R., et al., 2009, *A&A*, 502, 239